Spectral behavior of anomalies in deep metallic gratings

E. Popov and L. Tsonev

Institute of Solid State Physics, Bulgarian Academy of Sciences, Boulevard Lenin 72, Sofia 1784, Bulgaria

E. Loewen

Milton Roy Company, Analytical Products Division, 820 Linden Avenue, Rochester, New York 14625

E. Alipieva

Institute of Electronics, Bulgarian Academy of Sciences, Boulevard Lenin 72, Sofia 1784, Bulgaria

Received July 29, 1989; accepted March 30, 1990

An experimental investigation of spectral dependence of two recently discovered anomalies in deep metallic gratings is presented. Good coincidence with theoretical results is obtained. It is shown that the Brewster effect in deep gratings is suppressed with a decrease of wavelength, as the angle of incidence approaches zero. At the same time the groove-depth interval widens, and low values of reflectivity are observed.

1. INTRODUCTION

Two new types of anomaly in deep metallic gratings were recently discovered:

(i) Total absorption of light (TAL) in grazing incidence by an aluminum grating supporting two diffraction orders[1] has been explained as being directly connected to other types of anomaly of a plane metal–air boundary.[2,3]

(ii) Further investigations showed that the Brewster effect[4,5] exists also in deep gratings.[6]

The aim of this paper is to present both experimental and theoretical results on spectral dependence of these anomalies. Our interest is determined by the importance of TAL in surface-enhanced Raman scattering by gratings[7,8] and rough surfaces,[9] in some nonlinear phenomena,[10–14] in surface-plasmon luminescence,[15] and in solar absorbers.[16] Similar to TAL in shallow gratings,[4,5] TAL in deep gratings is observed if the trajectory of the zero α_0^z of the zeroth reflected order (ZZRO) in the complex α plane crosses the real axis (where $k\alpha$ is the wave-vector component that is parallel to the grating plane, $k = 2\pi/\lambda$ is the wave number, and λ is the wavelength). In the case of a single reflected order, namely, the specular one, this phenomenon is called the Brewster effect in gratings. Section 3 contains results on the spectral behavior of this anomaly in deep gratings. Below some critical wavelength value, TAL is suppressed. Close to cutoff, low values of reflectivity are observed over a large groove-depth interval; this is a result of practical interest because high groove-depth sensitivity is a strong limitation to the usefulness of TAL in shallow gratings.

If two orders (0 and −1) are permitted, the ZZRO usually causes blazing in the −1 order. But under certain conditions the −1 order can also vanish for almost all angles of incidence (antiblazing of gratings[17]) and, in particular, for the angle corresponding to the ZZRO. Thus TAL can be observed in a grating supporting two diffraction orders. Section 4 presents some results on the spectral dependence of these conditions.

2. EXPERIMENTAL SETUP

A. Grating Fabrication

A special grating with period $d \approx 0.5$ μm was recorded interferometrically in a photoresist Shipley AZ1350 with an Ar^+ laser. Two pinholes were used as point sources. Conical beam diameters, with Gaussian intensity distribution in the plane of interference, were slightly larger than the grating blank, the latter having a diameter of 47 mm.

As a result groove depths became highly nonuniform in a radial direction, with a maximum depth in the center. The appropriate exposure-development process provided a grating profile that was close to sinusoidal.[18] The developed resist was coated with a 200-nm-thick aluminum layer.

B. Local Groove-Depth-Values Reconstruction

As a first step of the experiment, determination of the groove-depth-value distribution along the principal diameter (i.e., perpendicular to the groove direction) of the grating is necessary. It is achieved indirectly by a comparison of local measurements of −1-order diffraction efficiencies (Fig. 1) with their theoretically calculated groove-depth dependences under the same conditions (Fig. 2). The final result of such a procedure is presented in Fig. 3 and permits the investigation of grating properties at different groove depths simply by the precise spatial positioning of the incident laser beam.

The measurements are performed for different polarizations and wavelengths (at $\lambda = 632.8$ nm and 514.5 nm in a Littrow mount and at $\lambda = 457.9$ nm at normal incidence) in order to increase the reliability of the method. Focusing the laser beam, we could select small surface regions, inside

0740-3232/90/091730-06$02.00

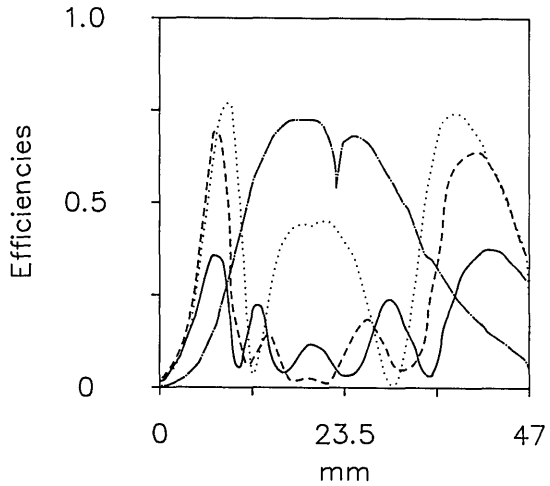

Fig. 1. −1-diffraction-order efficiencies distribution along the principal diameter of the grating: solid curve, $\lambda = 457.9$ nm, TM polarization, normal incidence; dashed curve, $\lambda = 514.5$ nm, TM polarization, Littrow mount; dotted curve, $\lambda = 632.8$ nm, TM polarization, Littrow mount; border curve, $\lambda = 632.8$ nm, TE polarization, Littrow mount.

which the groove depth could be kept almost constant. The set of angles of incidence included in the beam in this way does not exceed 0.06 deg. For such a small angular deviation, variations of the efficiencies presented in Figs. 1 and 2 are negligible.

Numerical calculations of the groove-depth dependences were performed for sinusoidal groove profile and were based on the differential formalism of Chandezon *et al.*,[19] which proved to be efficient and applicable for the groove depth to period ratio $h/d > 1$. Asymmetry of the real profile was neglected as the experiment showed a less than 1% difference between efficiency values measured symmetrically with respect to the grating normal.

The central region of the grating, between 16 and 25 mm, is overdeveloped; i.e., groove bottoms touch the glass substrate, and no further use of this region is made.

C. Laser Source for Spectral Measurements

As the phenomena that are to be investigated have strong angular sensitivity,[1-6] it is almost impossible to use a monochromator with a lamp source. For that reason we have chosen a continuous-wave dye laser instead. Two dyes, R6G and R6G (pH = 4.0), were employed to cover the spectral region used in the described experiment from 540 to 630 nm with a linewidth of 0.03 nm. In order to broaden the spectral range, we also used He–Ne–laser ($\lambda = 632.8$ nm), Kr^+-laser (647.1 and 676.4 nm), and Ar^+-laser (514.5 nm) lines.

3. BREWSTER EFFECT IN DEEP GRATINGS

If a plasmon surface wave propagates along a corrugated metal–air boundary, the trajectory of its propagation constant in the complex α plane forms loops if the groove depth is varied, provided that the wavelength-to-period ratio ensures radiation order(s) in the upper medium.[2,6] These loops are connected with the periodicity of diffraction properties of gratings as a function of groove depth and can also be explained with a formation of loops in the trajectories of ZZRO [Fig. 4(a)]. As a direct consequence, the Brewster effect in gratings can be observed at different groove-depth values as the trajectory of the zero consecutively crosses the real α axis. Figure 5 shows good coincidence between theoretically predicted and measured angular dependence of reflectivity for different groove-depth values corresponding to different parts of the zero trajectory of Fig. 4(a). Because the loop lies close to the real axis, low values of the reflectivity minimum exist over a large groove-depth range (Fig. 6). A small discrepancy between theoretical and experimental results can be understood in part by taking into account the fact that the measurements were performed by using either a collimated beam of finite spatial width (1 mm) or a focused beam of finite angular width (0.06 deg); thus the appropriate groove depth and angular condition cannot be achieved simultaneously.

As the wavelength is reduced, the incidence angle value corresponding to TAL approaches zero. On one hand the

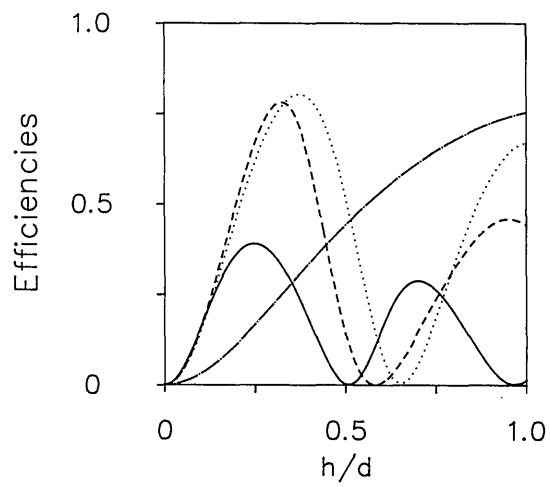

Fig. 2. Theoretical groove-depth dependence of −1-order diffraction efficiencies of sinusoidal aluminum grating (refractive index $1.09 + i5.01$) covered with 2.5-nm-thick layer of Al_2O_3 (refractive index 1.538), period $d = 500$ nm. Different curves correspond to the set of parameters of Fig. 1.

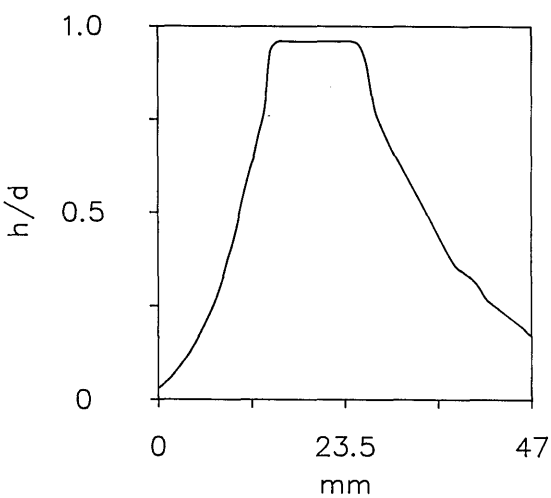

Fig. 3. Groove-depth-values distribution along the principal diameter of the grating: numerical reconstruction using data presented in Figs. 1 and 2.

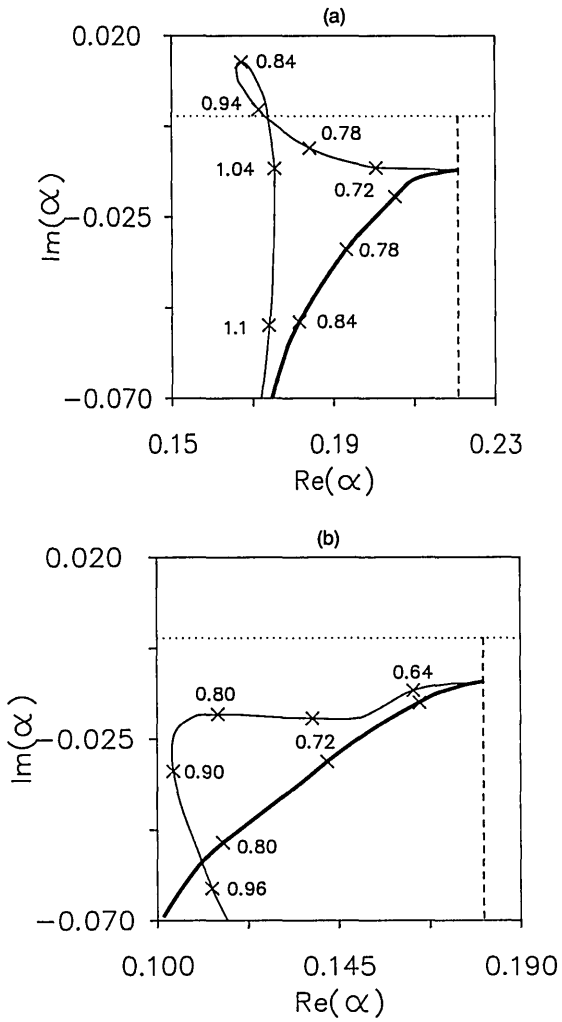

Fig. 4. Trajectories of the pole (thick solid curve) and the zero (solid curve) of the zeroth reflected order in the complex α plane for TM polarization and different groove-depth-to-period ratios (shown with crosses): dashed line, the −1-order cut; dotted line, real α axis. (a) $\lambda = 612.4$ nm; (b) $\lambda = 590.4$ nm.

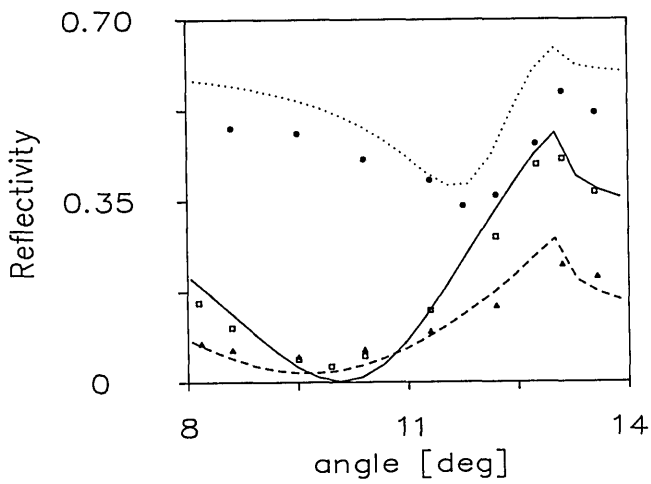

Fig. 5. Angular dependence of the reflectivity for different groove-depth values: dotted curve and circles, $h/d = 0.70$; solid curve and squares, $h/d = 0.82$; dashed curve and triangles, $h/d = 0.94$. The curves represent the theoretical results; the points represent the experimental ones. $\lambda = 612.4$ nm.

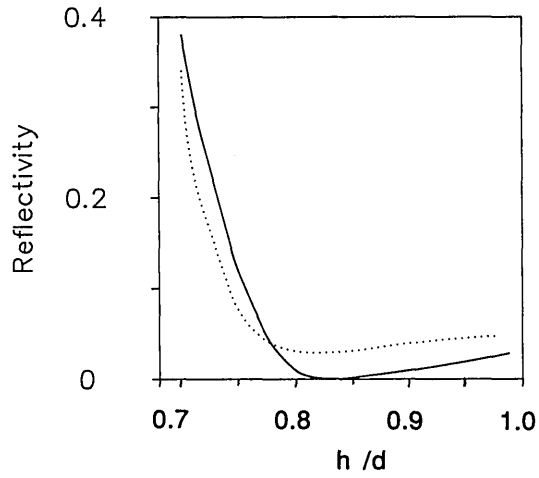

Fig. 6. Experimental (dotted curve) and theoretical (solid curve) values of reflectivity minimum presented in Fig. 5 as a function of groove depth. $\lambda = 612.4$ nm.

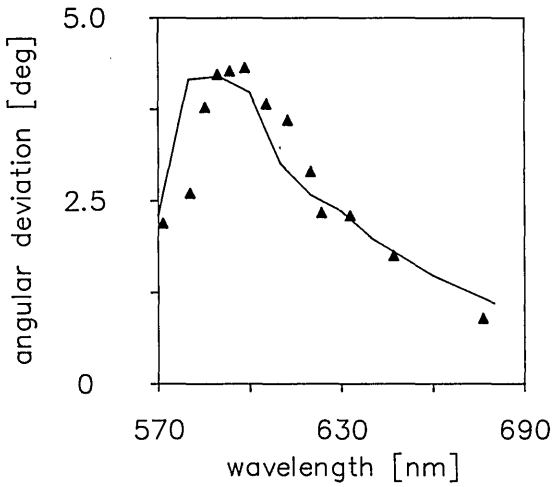

Fig. 7. Spectral dependence of angular deviation from the −1-order cutoff of reflectivity minimum position (Fig. 5). The triangles represent the experimental results; the solid curve represents theoretical ones.

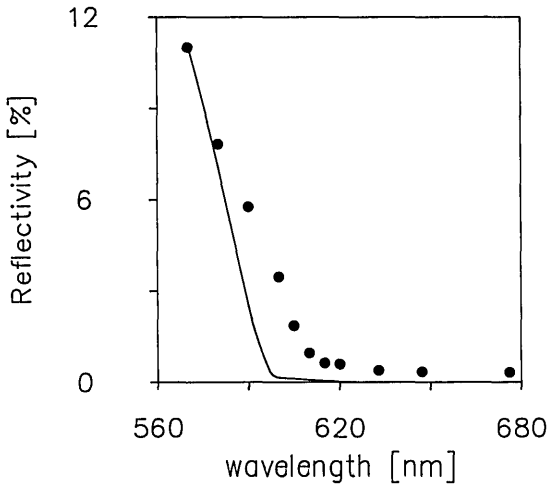

Fig. 8. Spectral dependence of the minimum reflectivity values. The circles represent the experimental results; the solid curve represents the theoretical ones.

TAL is going away from the −1-order cutoff represented by dashed lines in Fig. 4. For λ decreasing toward 595 nm, the angular deviation in Fig. 7 increases. On the other hand the −1-order cutoff itself moves toward Re(α) = 0 with decreasing λ (Fig. 4). Approaching normal incidence, interaction among plasmons propagating in different directions becomes stronger. As a result stronger repelling of poles and zeros takes place.[20–22] Below some critical wavelength value the trajectory of the ZZRO lies totally under the real α axis [Fig. 4(b)], and we can expect suppression of the TAL.[23]

The experiment closely confirms these theoretical conclusions for $\lambda < 595$ nm, as is shown in Fig. 8.

4. GRAZING INCIDENCE ANOMALY

The TAL in grazing incidence[1] by a grating supporting two diffraction orders is exhibited if two different phenomena are observed simultaneously:

(i) Vanishing of the −1 diffraction order in the Littrow mount happens if the groove-depth value is appropriately chosen. In that case −1-order efficiency is negligible almost everywhere,[17] and the grating acts as a plane mirror. The optimal groove-depth-to-period ratio varies slightly with wavelength and remains close to 0.7 (Fig. 9).

(ii) The case of zero of the ZZRO is contrary to the case discussed in Section 3, in which the ZZRO trajectory exists separately and simultaneously with the polar trajectory (Fig. 4). Now the zero trajectory is a continuation of the pole trajectory at the other side of zeroth-order cutoff for higher groove-depth values (Fig. 10). A detailed analysis of the first cross point with the real α axis [Fig. 10(a)], resulting in the so-called non-Littrow perfect blazing, can be found in Refs. 24–26. Here we are interested in the second cross point denoted in Fig. 10(a) by α^z_{II}.

In the spectral interval of $1.1 < \lambda/d < 1.5$, this ZZRO is exhibited at high angles of incidence θ. If angular conditions are not properly satisfied (i.e., $\sin\theta \neq \alpha$), a minimum rather than a pure zero is observed in the groove-depth dependence of the zeroth-order efficiency. For different angles of incidence this minimum in the reflectivity is exhibited at different groove-depth values corresponding to different parts of the zero trajectory that lie nearest to $\alpha = \sin\theta$, even for the same wavelength value. The results for spectral dependence of optimal groove-depth values are presented in Fig. 9 for three different angles of incidence. Good agreement between experimental and theoretical results is observed.

An expanded and collimated laser beam covers the whole grating blank. The value of the angle of incidence is determined by measuring the linear separation of the transmitted and reflected beams at a distant screen. Two dark lines in the zeroth-order reflected beam that is shown in Fig. 11a correspond to the groove-depth regions responsible for a minimum of reflectivity. The intensity distribution of the image area is analyzed by a computer-controlled 256-element photodetector array. The results are shown in Fig. 11b. Operating in the saturated registration regime (Fig. 11c) enables us to determine precisely the position of the two dark lines on the principal grating diameter and, hence, to reconstruct the corresponding groove-depth values by using the results of Fig. 3.

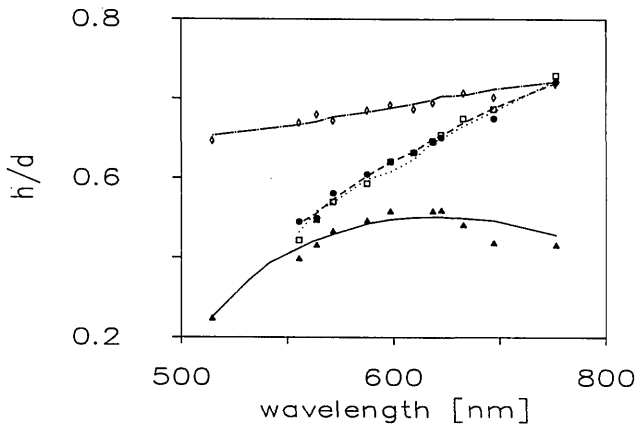

Fig. 9. Spectral dependence of the optimal groove-depth values corresponding to the minimum in diffraction efficiencies of the −1 diffraction order (dashed–dotted curve and rhombs) in Littrow mount and 0 diffraction order at angles of incidence $\theta = 75°$ (solid curve and triangles), $\theta = 85°$ (dotted curve and squares), and $\theta = 87.5°$ (dashed curve and circles). The curves represent the theoretical results; the other symbols represent the experimental ones.

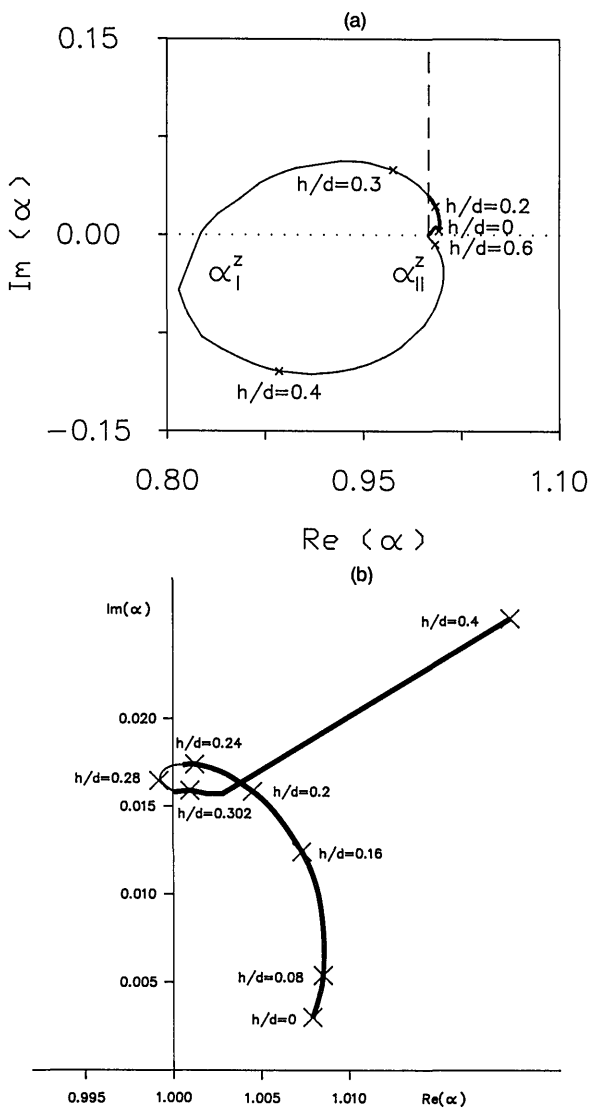

Fig. 10. Trajectory of the pole (thick solid curve) and the zero (solid curve) of the zeroth diffraction order in the complex α plane for TM polarization and different values of h/d: (a) $\lambda = 632.8$ nm; (b) $\lambda = 520$ nm (Ref. 1).

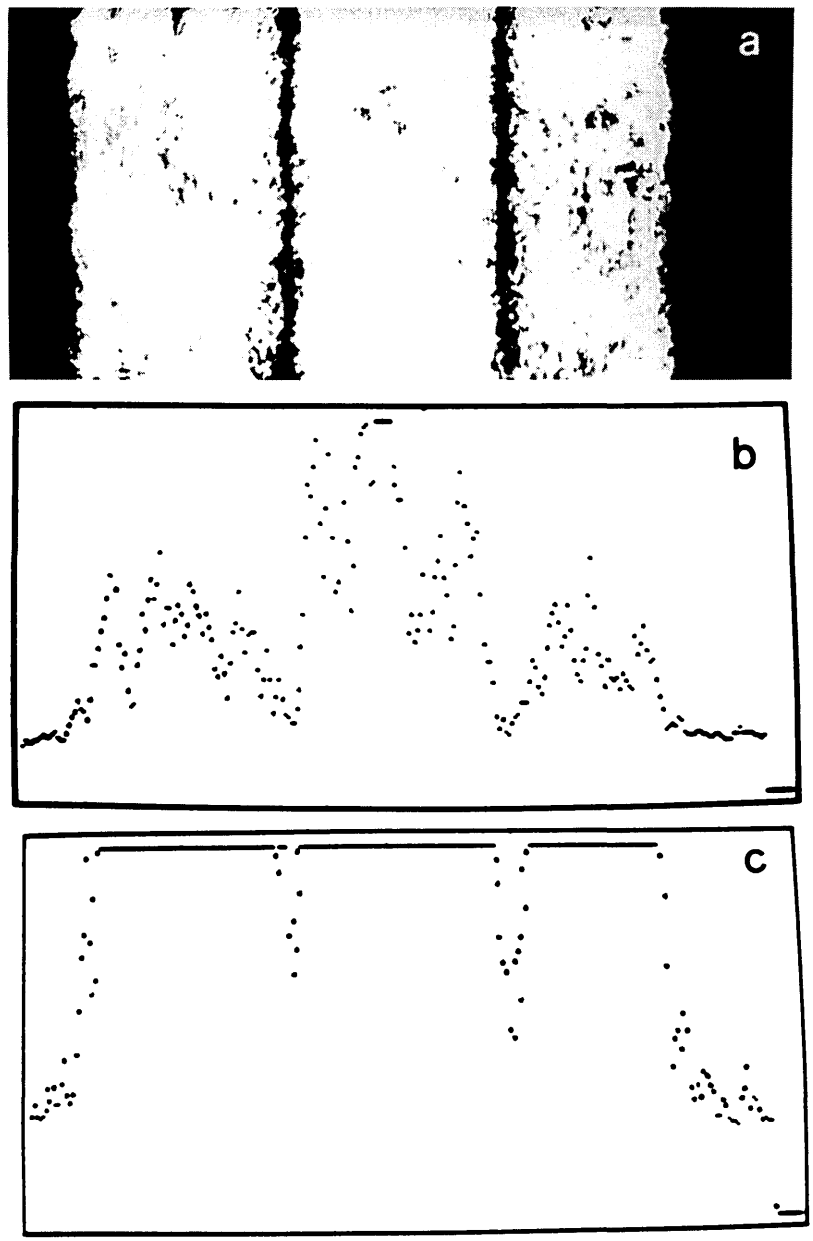

Fig. 11. Light intensity distribution of the zeroth reflected order at a high angle of incidence $\theta = 85^{+}$ using expanded and collimated source beam: a, the spot picture; b, the distribution measured by a computer-controlled detector array; c, the distribution measured in the saturated registration regime.

Going back to Fig. 9, some interesting conclusions concerning the grazing incidence anomaly can be drawn. For longer wavelengths, the groove-depth value corresponding to the minimum of the zeroth-order efficiency at high incidence angles comes close to, and finally coincides with, the groove depth value connected with -1 efficiency minimum. At the same time, as $\sin\theta \approx \alpha_{II}^{z}$, the value of the zeroth-order efficiency minimum becomes very low. Thus near-TAL by a grating supporting two diffraction orders is observed under a specific combination of groove-depth, wavelength, and angle-of-incidence values.

If the wavelength is reduced, the reflection minimum moves toward shallower grooves (Fig. 9). At the same time its angular position shifts toward lower angles of incidence. The loop in the ZZRO trajectory in the complex α plane shrinks; below some critical wavelength value ($\lambda \approx 530$ nm) it lies totally above the real α axis [Fig. 10(b)], and its influence on the reflectivity is diminished. Therefore, at high angles of incidence a minimum in the reflectivity cannot be detected for shorter wavelengths (Fig. 9).

REFERENCES

1. L. Mashev, E. Popov, and E. Loewen, "Total absorption of light by a sinusoidal grating near grazing incidence," Appl. Opt. **27**, 152–154 (1988).
2. E. Popov, L. Mashev, and E. Loewen, "Total absorption of light

by gratings in grazing incidence: a connection in the complex plane with other types of anomalies," Appl. Opt. **28,** 970–977 (1989).
3. L. Mashev and E. Popov, "Anomalies of metallic diffraction gratings," J. Opt. Soc. Am. A **6,** 1561–1567 (1989).
4. D. Maystre and R. Petit, "Brewster incidence for metallic gratings," Opt. Commun. **17,** 196–200 (1976).
5. M. C. Hutley and D. Maystre, "Total absorption of light by a diffraction grating," Opt. Commun. **19,** 431–436 (1976).
6. L. Mashev, E. Popov, and E. Loewen, "Brewster effect in deep metallic gratings," Appl. Opt. **28,** 2538–2541 (1989).
7. K. Metcalfe and R. Hester, "Raman scattering from thin polystyrene films on gold diffraction gratings," Chem. Phys. Lett. **94,** 411–415 (1983).
8. M. Yamashita and M. Tsuji, "Simple theory for surface plasmon-polariton resonance on sinusoidal metal surface: application to SERF," J. Phys. Soc. Jpn. **52,** 2462–2471 (1983).
9. R. Renisch and M. Nevière, "Increase in Raman excitation of surface polaritons with surface roughness explained in terms of Wood anomalies of gratings," Opt. Eng. **20,** 629–633 (1981).
10. D. Maystre, M. Nevière, M. Renisch, and J. L. Coutaz, "Integral theory for metallic gratings in nonlinear optics and comparison with experimental results on second-harmonic generation," J. Opt. Soc. Am. B **5,** 338–351 (1988).
11. M. Nevière and R. Reinisch, "Electromagnetic theory of enhanced nonlinear optical process," J. Phys. (Paris) **44,** C10-349–361 (1983).
12. R. Reinisch, G. Chartier, M. Nevière, M. C. Hutley, G. Causs, J. P. Galaup, and J. F. Eloy, "Experiment of diffraction by a nonlinear grating in nonlinear optics: second harmonic generation," J. Phys. Lett. Paris **44,** L-1007–1009 (1983).
13. J. L. Coutaz, "Experimental study of second-harmonic generation from silver gratings of various groove depths," J. Opt. Soc. Am. B **4,** 105–106 (1987).
14. M. Nevière, H. Akhouayri, P. Vincent, and R. Reinisch, "Surface enhanced second harmonic generation in dielectric deposited over a silver grating, in *Application and Theory of Periodic Structures, Diffraction Gratings, and Moiré Phenomena III,* J. M. Lerner, ed., Proc. Soc. Photo-Opt. Instrum. Eng. **815,** 146–152 (1987).
15. J. L. Coutaz and R. Reinisch, "Groove depth dependence of surface plasmon luminescence from base silver gratings," Solid State Commun. **56,** 545–548 (1985).
16. See, for example, *Electromagnetic Theory of Gratings,* R. Petit, ed. (Springer-Verlag, Berlin, 1980), Chap. 7.
17. L. Mashev, E. Popov, and D. Maystre, "Antiblazing of gratings," Opt. Commun. **67,** 321–324 (1988).
18. L. Mashev and S. Tonchev, "Formation of holographic diffraction gratings in photoresist," Appl. Phys. A **26,** 143–149 (1981).
19. J. Chandezon, M. Dupuis, G. Cornet, and D. Maystre, "Multicoated gratings: a differential formalism applicable in the entire optical region," J. Opt. Soc. Am. **72,** 839–846 (1982).
20. E. Popov, L. Tsonev, and D. Maystre, "Gratings-general properties in Littrow mount and energy flow distribution," J. Mod. Opt. **37,** 367–378 (1990).
21. E. Popov, L. Tsonev, and D. Maystre, "Losses of plasmon surface wave on metallic gratings," J. Mod. Opt. **37,** 379–383 (1990).
22. E. Popov, "Plasmon interactions in metallic gratings: w- and k-minigaps and their connection with poles and zeros," Surf. Sci. **222,** 517–527 (1989).
23. E. Popov, "Total absorption of light in metallic gratings: a comparative analysis of spectral dependence for shallow and deep grooves," J. Mod. Opt. **36,** 669–676 (1989).
24. D. Maystre, M. Cadilhac, and J. Chandezon, "Gratings: a phenomenological approach and its applications, perfect blazing in non-Littrow mounting," Opt. Acta **28,** 457–470 (1981).
25. D. Maystre and M. Cadilhac, "A phenomenological theory for gratings: perfect blazing for polarized light in nonzero deviation mounting," Radio Sci. **16,** 1003–1010 (1981).
26. M. Breidne and D. Maystre, "One hundred percent efficiency of gratings in non-Littrow configurations," in *Periodic Structures, Gratings, Moiré Patterns, and Diffraction Phenomena I,* C. H. Chi, E. G. Loewen, and C. L. O'Bryan III, eds., Proc. Soc. Photo-Opt. Instrum. Eng. **240,** 165–170 (1980).